Journal of Materials Science and Engineering A 5 (9-10) (2015) 339-350
doi: 10.17265/2161-6213/2015.9-10.003

Formation of Al/Au Bimetallic Interface Studied by Angle-Resolved X-Ray Photoelectron Spectroscopy (ARXPS)

Yaroslav Polyak

Institute of Physics, Academy of Sciences of the Czech Republic, CZ-18221 Prague 8, Czech Republic

Abstract: ARXPS (Angle-resolved X-ray photoelectron spectroscopy) measurements were performed on the thin aluminum films deposited on the gold polycrystalline substrate kept at the temperature of liquid nitrogen in order to characterize the interdiffusion process during early stages of Al/Au interface formation. The intermixing of Al and Au elements at Al/Au bimetallic interface occurred already at temperature of liquid nitrogen leading to the formation of the well-resolved component on the high binding energy side of Au(4f) core line corresponding to AlAu intermetallic phase. The formation of initial AlAu phase at Al/Au interface in our experimental conditions can be explained on the base of its thermodynamic stability. The sample annealing resulted in the growth of the amount of AlAu intermetallic compound formed at liquid nitrogen temperature with subsequent decomposition of the parent alloy phase and formation of $AlAu_2$ intermetallics richer in Au atoms. Tikhonov regularization method was used to extract the aluminum in-depth concentration profile from the measured ARXPS intensities. L-curve analysis was applied to determine the regularization parameter.

Key words: ARXPS (Angle-resolved X-ray photoelectron spectroscopy), Al/Au interface, Au(4f) doublet, phase transformations, concentration profile.

1. Introduction

The Au-Al system has been extensively studied especially due to its application in the microelectronic industry [1-9]. Miniaturization of device dimensions provides an increase of signal propagation speed and lower power dissipation. However, good device performance requires low resistance contacts and interconnections. The high integration, high functionality and downsizing of electronic devices emphasize the importance of the bonding interface. Frequent unreliability of the Al-Au joints is associated with the stability of their mechanical and electrical properties. At high temperature working conditions, it is common that the wire bonding degrades due to the growth of the Al-Au intermetallics. The formation of the intermetallics makes the bonds stronger but more brittle and mechanically stressed owing to the volumetric changes of intermetallics in comparison with pure Au and Al materials [1-5].

There are numerous studies of the phase formations in Al-Au bilayer couples (Al (50 nm ~ 1 μm), Au (200 nm ~ 1 μm)) at elevated temperatures (45 ~ 600 °C) using RBS (Rutherford backscattering spectroscopy), XRD (X-ray diffraction) technique and TEM (Transmission electron microscopy) [6-9]. The authors [5-8] have reported that the first phase formed at the Al/Au interface was Al_2Au_5 and/or $AlAu_2$ intermetallics. This result is in agreement with the phase selection rule proposed by Pretorius [10]. The rule combines thermodynamic and kinetic factors and is based on the so-called "effective heat of formation". Indeed, Al_2Au_5 and $AlAu_2$ have similar effective heats of formation which are significantly larger than those of other Al_xAu_y compounds [10].

The Au_xAl_y alloys are characterized by considerable shifts of Au(4f) core level binding energy position with the change of phase, so XPS (X-ray photoelectron

*Corresponding author: Yaroslav Polyak, associated scientist, research fields: surface science and thin solid films.

spectroscopy) provides a suitable means to follow intermetallics formations at the Al/Au interface [11-13]. However, it should be kept in mind that the information depth of XPS method is only few nanometers.

Angle-resolved XPS (ARXPS) is currently used for the determination of the in-depth concentration profile nondestructively in the sample sub-surface region. In this method, the analyzing depth is varied by changing the detection angle of photoelectrons. In practice, the in-depth profile restoration is associated with a discrete linear inverse problem. The inverse problem, in turn, belongs to the class of the so-called ill-posed problem, which means that the solution is not unique or is not a continuous function of the data. Because a real signal always contains noise, there is no unequivocal assignment of the angle-dependent spectral intensities to the sub-surface concentration profile. There are numerous algorithms to extract the in-depth profiles using ARXPS data ranging from the various fitting procedures and Laplace transforms to the regularization routines. These methods are discussed in the review paper by Cumpson [14]. Among all these methods, Tikhonov regularization has proved to be a powerful technique in many fields of the information restoration. It suppresses the unwanted noise components and overcomes the problems associated with the numerical instabilities [15].

In spite of many challenges with the data interpretation, ARXPS provides a reliable means for the identification of various bimetallic phases via measurements of the core-level binding energy shifts of photoelectrons and extraction of the in-depth concentration profile at the sample surface. ARXPS is a very powerful method to study the bimetallic systems in which processes such as alloying, reactive diffusion, surface segregation, cluster formation occurs. In this research, the diffusion of Al into Au substrate is investigated using ARXPS method with the emphasis on the initial stages of the Al/Au interface formation. In general, the deposition of one metal on the surface of another metal kept at low temperatures leads to a metastable configuration. The metastable state supresses the diffusion and growth processes due to the existence of activation barriers. Heating usually causes the energetic barriers to be surmounted and system lowers its free energy through intermixing and alloying.

2. Experimental Details

The different amounts of Al were vapour-deposited onto the flat polycrystalline Au substrate in the preparation chamber of VG ESCA 3 Mk II photoelectron spectrometer. Prior to Al deposition, the surface of Au foil was cleaned using mild Ar^+ ion sputtering procedure (E_k = 3 KeV, P = 5 × 10^{-5} mbar, t = 15min). The survey photoelectron spectra did not reveal the traces of the surface contaminants confirming the cleanliness of the sample surface during our experiments. The depositions were performed using a home-made evaporator constructed from a high purity (99.999%) aluminium foil wrapped around tungsten coil. The outgassed tungsten coil was heated by the direct current enabling Al atoms to sublimate. The distance between the evaporator and the substrate was sufficiently large to produce a thin layer of constant thickness with the deposition rate of 10 Å/min. UHV (Ultra-high vacuum) conditions in the preparation chamber were better than 10^{-8} Pa in the course of Al depositions. The sample thermal treatments from the temperature of liquid nitrogen up to 100 $^{\circ}$C were performed using the specially designed cooling/heating system attached to the substrate holder.

The ARXPS measurements were carried out immediately after Al deposition without breaking the vacuum. The photoemission spectra of Au(4f) and Al(2p) electrons were recorded at the detection angles of 25°, 45° and 65° measured from the sample surface normal. The non-monochromatic Al Kα (1486.6 eV) radiation was used to excite the core-level electrons. The hemispherical electron analyser was operated in the constant energy mode at pass energy of 20 eV. The binding energies were calibrated by setting up the

analyser to give Au ($4f_{7/2}$) line position of 84.0 eV for a metallic gold.

Al vapour deposition on bare Au substrate cooled by liquid nitrogen resulted in the alloy formation between Al and Au materials. In order to investigate the evolution of the thermally activated processes occurring at Al/Au interface, the stepwise heating procedure from liquid nitrogen up to the room temperature was carried out. During the sample annealing a solid-solid diffusional reaction is expected to evolve to a great extent. It means that signal intensities from $Au(4f)_{met}$, $Au(4f)_{alloy}$ and Al(2p) components varied significantly in the course of the sample heating. To arrest the Al-Au diffusion-reaction, the sample was cooled down to the liquid nitrogen temperature after each step of the annealing and then ARXPS data were collected. Keeping the sample at the temperature of liquid nitrogen enabled to obtain the equivalent spectral scans during the data acquisition for several minutes.

Prior to the decomposition of Au(4f) and Al(2p) envelopes into the individual components, X-ray satellites produced by the non-monochromatic Al Kα radiation were removed from the recorded XP spectra [16]. The integrated peak intensities and peak positions were obtained applying NLLSF (Nonlinear least-square fitting) and Shirley-type background subtraction procedure [17]. The theoretical values of the photoionization cross section of Scofield [18] and IMFP (Inelastic mean free path) of photoelectrons of TPP-2M [19] were used in the concentration profile calculations.

3. Results and Discussion

3.1 Intermetallic Growth and Phase Transformations

After Al deposition on Au polycrystalline foil kept at the temperature of liquid nitrogen, Au(4f) doublet was resolved into two pronounced individual doublets spaced 1.5 eV apart and having approximately the equal values of FWHM (Full width at half maximum) (Fig. 1). Obviously, Au(4f) doublet positioned at lower binding energy corresponds to the metallic Au of the substrate. The binding energy shift (~ 1.5 eV) of $Au(4f_{7/2})$ line of the alloy phase formed at Al/Au interface is close to the value corresponding to the bulk AlAu intermetallic [11-13]. The formation of AlAu bimetallic phase at Al/Au interface at the temperature of liquid nitrogen can be explained on the base of its thermodynamic stability [20].

The intermetallic compound growth in the binary system is a process involving mutual interdiffusion of both elements across the bimetallic interfaces. From a general point of view, AlAu alloy layer grows due to two partial chemical reactions at its interfaces: the Al atoms diffuse across AlAu layer to react with the Au atoms and the Au atoms diffuse across AlAu layer in the opposite direction to react with Al atoms.

Due to the different sizes of Al and Au atoms and melting points of Al and Au metals, the contributions of these reactions to the alloy growth process can hardly be expected to be equal. Indeed, the atomic radius of Al (0.143 nm) is smaller than that of Au (0.174 nm) and Al metal has considerably lower melting point of 660 °C in comparison with 1,064 °C for Au metal [21]. In addition, vacancy formation energies for aluminium are significantly lower than those for gold in AlAu alloy, especially for gold-rich conditions [22]. Hence Al atoms are expected to diffuse more readily into AlAu thin layer than Au atoms becoming the dominant diffusing species in the growing AlAu intermetallics.

The calibrated and normalized Al(2p) and Au(4f) photoelectron spectra as a function of annealing temperature are shown in Fig. 2. The observed increasing tendency of $Au(4f)_{alloy}/Au(4f)_{metal}$ intensity ratio in the course of sample heating up to the room temperature is associated with the gradual growth of AlAu alloy.

After prolonged heating of the sample at the room temperature, Au(4f) peak position shifts to lower binding energy evidencing the transformation of AlAu alloy into the gold-richer $AlAu_2$ bimetallic phase as illustrated in

Fig. 3. At the same time, Al(2p) peak position shifts to the higher binding energies confirming the formation of the gold-richer $AlAu_2$ alloy phase.

The values of FWHM and BE (Binding energy) of $Au(4f_{7/2})$ peak corresponding to the Al_xAu_y alloy phase during prolonged heating of the sample up to 100 °C are graphically illustrated in Fig. 4. The variation of FWHM values is accompanied by the gradual decrease of BE position of Au(4f) line in the course of our experimental measurements. The observed significant broadening of Au(4f) peak is due to the presence of the different bimetallic phases in XPS monitored reaction zone. Obviously, the value of FWHM of Au(4f) envelope is determined by the relative weights of the strongly overlapping peaks of the adjacent Al_xAu_y alloy phases. In the end of the sample thermal treatment, the invariable value of BE position of $Au(4f_{7/2})$ core level and the narrowest FWHM of $Au(4f_{7/2})$ peak indicates the presence of single gold-richest intermetallic phase at the sample surface.

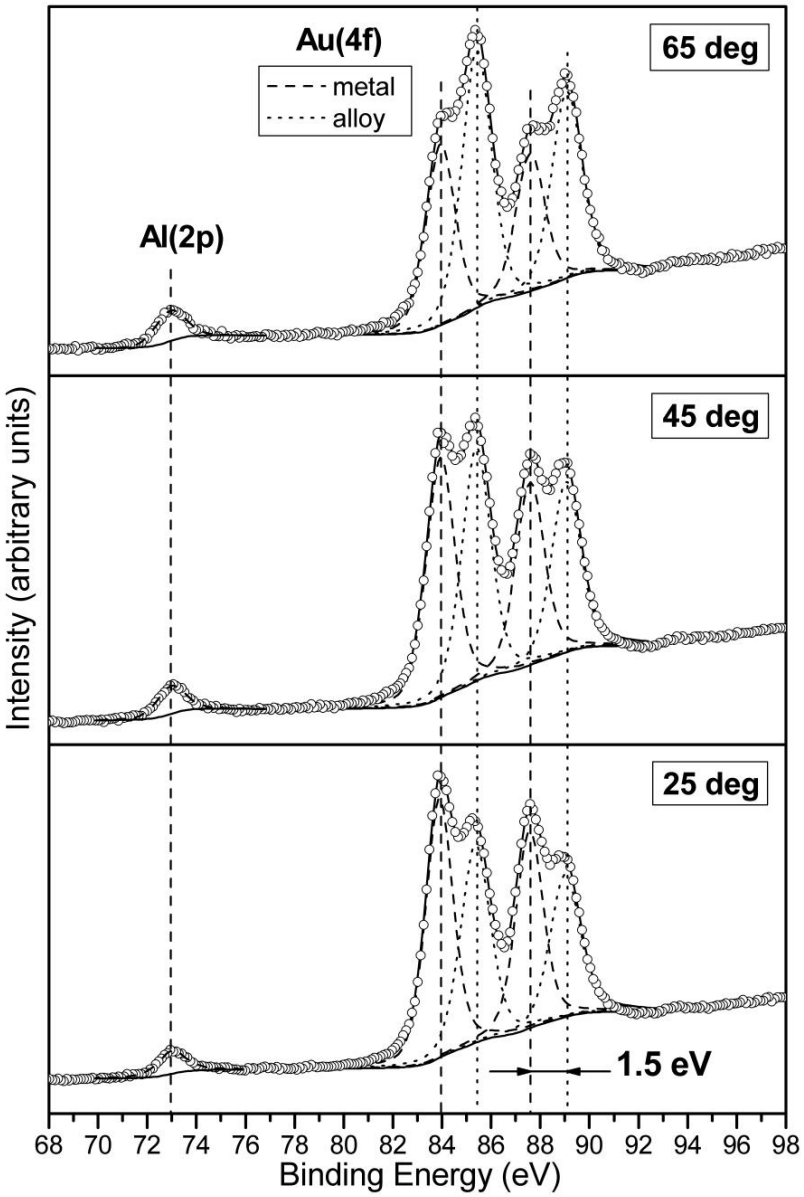

Fig. 1 Fitted spectra of Au(4f) and Al(2p) photoelectrons taken from Al film deposited on Au substrate kept at temperature of liquid nitrogen. The spectra were recorded at the detection angles of 25°, 45° and 65° measured from the surface normal.

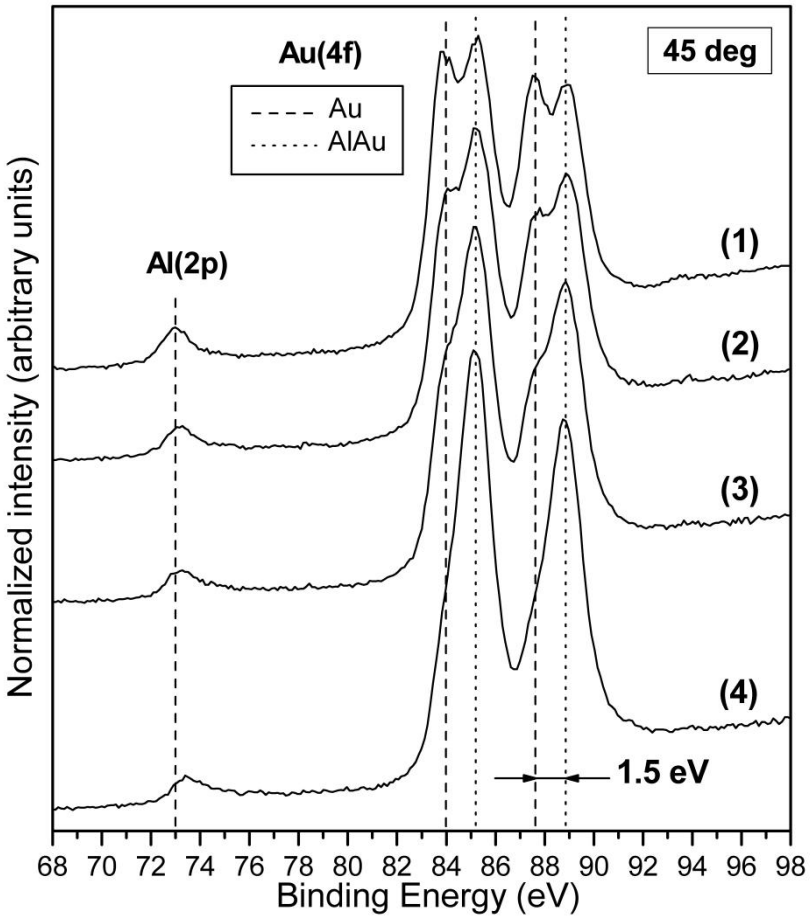

Fig. 2 Spectra of Au(4f) and Al(2p) photoelectrons recorded at detection angle of θ = 45° (measured from surface normal) from Al film deposited on the Au substrate kept at temperature of liquid nitrogen:
(1) After deposition at liquid nitrogen temperature; (2) After heating to − 100 °C and subsequent cooling to liquid nitrogen temperature; (3) After heating to − 100 °C for 10 min and subsequent cooling to liquid nitrogen temperature; (4) After heating to − 50 °C and subsequent cooling to liquid nitrogen temperature.

The following model is proposed to describe the thermally activated processes occurred at Al/Au interface in the course of the sample thermal treatments. The deposition of Al onto Au substrate leads to the formation of the bimetallic AlAu phase which grows during annealing. Owing to the limited supply of the elemental Al on the sample surface AlAu phase grows until the complete consumption of the elemental aluminium [23]. The rapid diffusion of the Al atoms into the gold substrate leads to the gradual decomposition of AlAu phase and subsequent formation and growth of the intermetallics richer in gold element. The parent AlAu alloy phase serves as a source of aluminium for the new-growing $AlAu_2$ alloy phase. In the final stage of the prolonged annealing of the sample, Al/Au interface can be considered on the base of the equilibrium phase diagram.

Another interesting aspect here is the phase propagations in the reaction zone which can be regarded on the base of the regular diffusion in the bimetallic couples implying that each Au-richer phase propagates with a planar interface through the preceding Au-poorer phase [24, 25]. However the fast transport of Al atoms along the grain boundaries prevents the formation of the planar boundary between the different phases. In this case the adjacent intermetallic compounds are mixed and dispersed throughout the reaction zone rather as a uniform homogeneous layer.

In fact, we have no direct experimental evidence

upon the distribution of the adjacent alloy phases in the reaction layer on the base of our ARXPS measurements. We suppose that the initial AlAu alloy phase grows accordingly to the homogeneous layer model due to the presence of the defects associated with the sample surface and created by Ar^+ bombardment which gradually saturate. In the next step, the reactive diffusion proceeds from the saturated defects into the interior of the grains by lattice diffusion leading to the overlapping of the diffusion field from the adjoining polycrystalline grains. As a result, the different phases are separated with a continuous boundary in the reaction zone.

3.2 Concentration Profile

In order to understand in greater detail the diffusion of Al deposit into Au substrate, the in-depth concentration profiles were calculated. In general, the

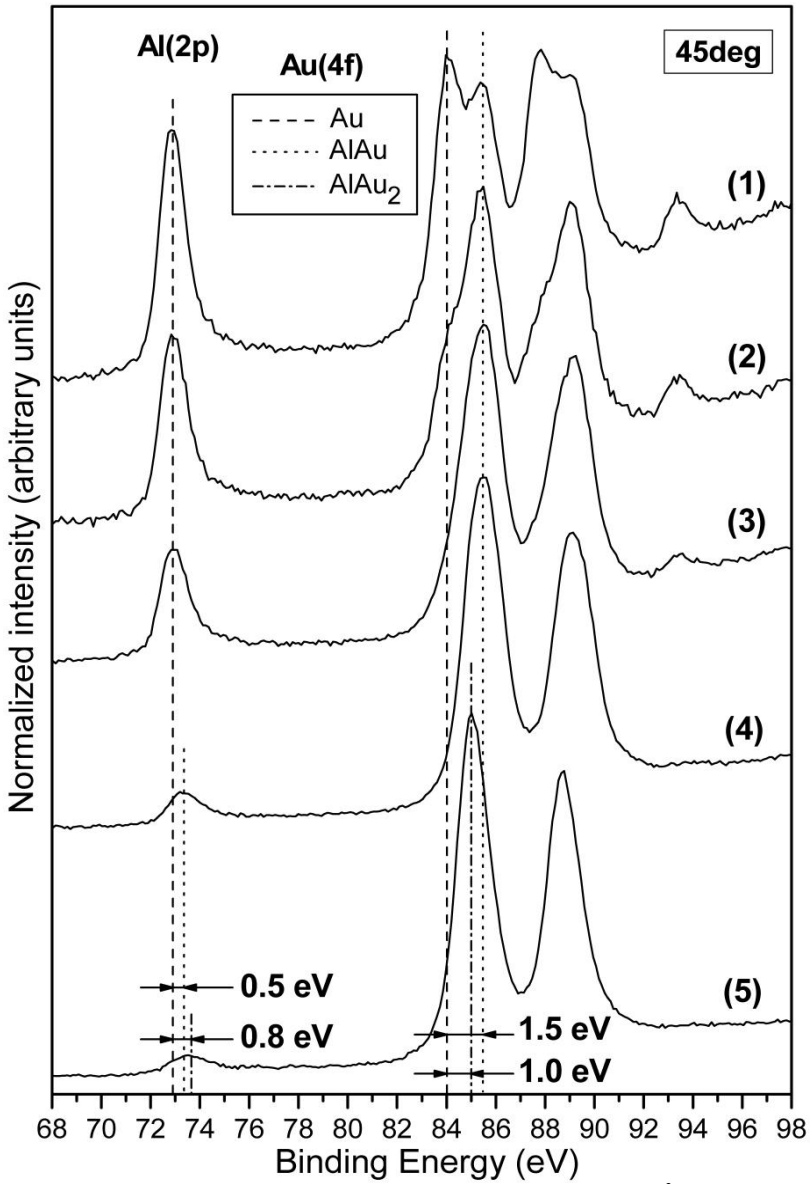

Fig. 3 Spectra of Au(4f) and Al(2p) photoelectrons recorded at detection angle of θ = 45° (measured from the surface normal) from Al film deposited on Au substrate:

(1) After deposition at liquid nitrogen temperature; (2) After heating to − 50 °C and subsequent cooling to liquid nitrogen temperature; (3) After heating to room temperature; (4) After prolonged (1,060 min) heating at room temperature; (5) After prolonged (1,860 min) heating at room temperature.

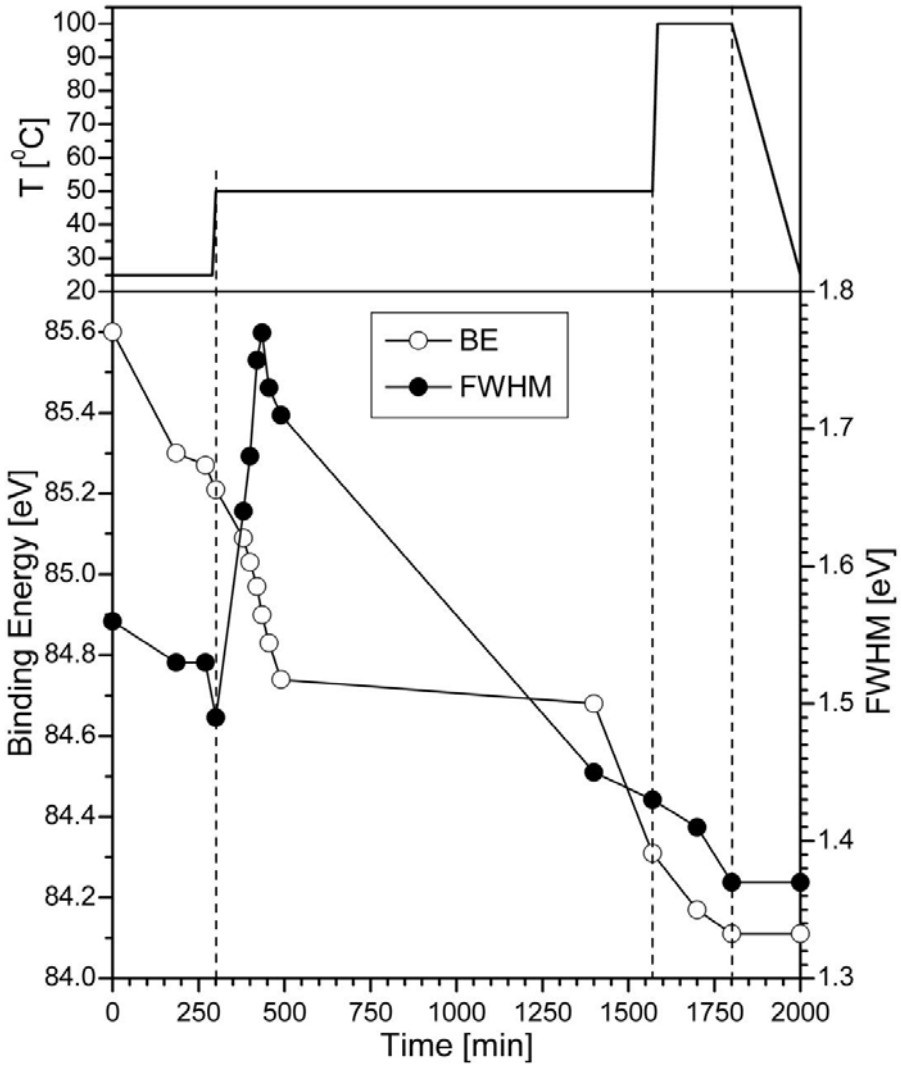

Fig. 4 Evolution of binding energy position and FWHM of Au($4f_{7/2}$) peak corresponding to alloy phase with time and temperature.

depth profiles were not obvious from inspection of ARXPS data. Furthermore, the real measured data contained noise. Other problems arised from sample roughness, electron refraction, elastic scattering and so on. In addition, the deep layers (> 3 nm) contribute weakly to the measured signal. There were a large number of the models in-depth profiles which produce the calculated data in the agreement with the experimental data within the precision of measurements. A simple optimization of the weighted sum of error squares between the calculated and measured data was not adequate to determine the correct concentration profile. Tikhonov regularization technique, which is not limited by the small number of the experimental data, was used to obtain the "robust" in-depth concentration profile in the near-surface sample region [14].

The Al concentration profile was calculated from the Au(4f) and Al(2p) peak intensities measured at the detection angles of 25°, 45° and 65° with respect to the surface normal after Al evaporation on Au polycrystalline substrate kept at temperature of liquid nitrogen (Fig. 5). The in-depth concentration profiles were also extracted after two stages of the sample thermal treatments - short heating at − 50 °C for several minutes and prolonged heating at the ambient temperature.

The layered sample model was applied to generate

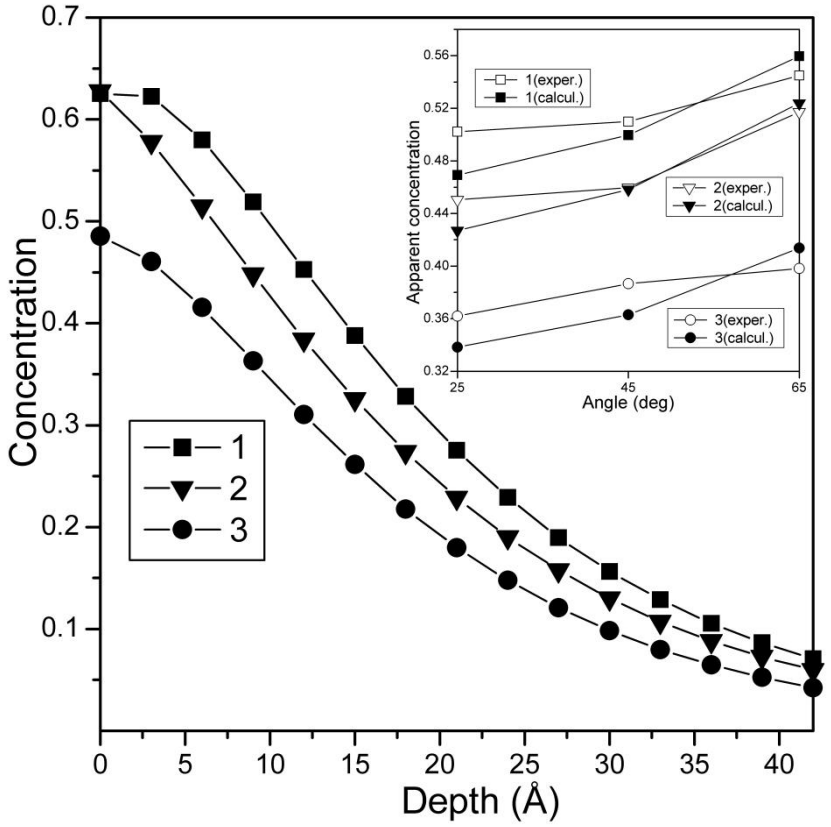

Fig. 5 Al in-depth concentration profile extracted from ARXPS data applying Tikhonov regularization and comparison between experimental (empty symbols) and calculated (filled symbols) values of the apparent atomic fractions as a function of the detection angle:

(1) After deposition at liquid nitrogen temperature; (2) After heating at − 50 °C; (3) After heating at room temperature.

XPS signal in the binary system [26, 27]. The effects due to the elastic scattering were not included in the model [28]. The following data were used in our calculations: theoretical values of photoionization cross-section published by Scofield [18]: $\sigma_{Al} = 0.54$, $\sigma_{Au} = 17.1$; number of layers N = 14; thickness of each layer t = 0.3 nm; values of IMFP were calculated from TPP-2M equation [19] for Al and Au photoelectrons transported in Au matrix: $\lambda_{Al} = 1.66$ nm, $\lambda_{Au} = 1.65$ nm. Tikhonov regularization was applied to obtain the "robust" in-depth profiles from the results of ARXPS measurements using matrix algebra without imposing of the constraints [29, 30]. The algorithm was implemented in MS Excel spreadsheets.

The regularization parameter α was optimized using the L-curve criterion [31, 32]. The L-curve is a very convenient graphical tool for the analysis of Tikhonov regularization. The typical graphical illustration of the L-corner region used in the in-depth profile restorations was shown in Fig. 6. The values of the regularization parameter used in our calculations of Al concentration profiles are in the range of 0.09 - 0.12.

In order to test stability and robustness of the obtained in-depth profiles, noise was added to the measured photoelectron peak intensities. Random data of the amplitude 10% of the measured signal were generated. The calculated concentration profiles do not display the significant deviation from the original dependences.

The reasonable agreements between the "calculated apparent concentration" obtained from the extracted in-depth profile and the "experimental apparent concentration" as a ratio of Al(2p) to Au(4f) peak areas were graphically illustrated in the top right corner

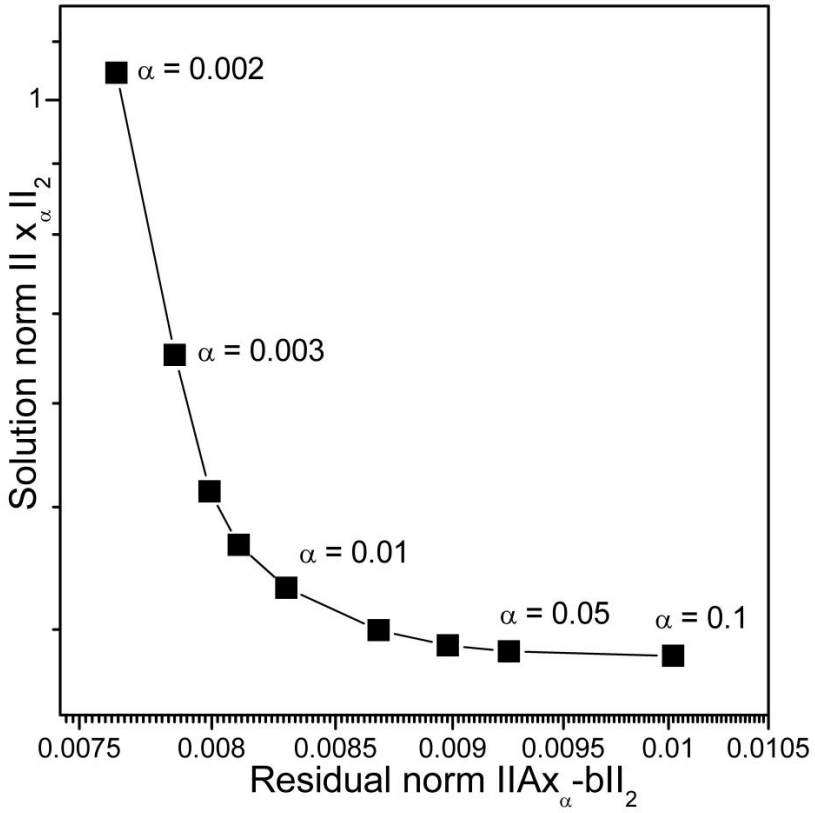

Fig. 6 Graphical illustration of the L-curve criterion (a log-log plot of the solution norm $\|x_\alpha\|_2$ versus the residual norm $\|Ax_\alpha - b\|_2$ with α as the parameter) used for the determination of the regularization parameter α in the Al in-depth profile reconstructions.

of Fig. 5. The "experimental apparent concentration" was corrected for the photoionization cross-section but not for IMFP.

In general, the volume diffusion process in a typical polycrystal was characterized by the lower diffusivity through the defect-free lattice and the higher diffusivity along the grain boundaries and was described by so-called isoconcentration curve as illustrated in Fig. 7 [33].

However, the real polycrystalline material consists of the microscaled grains of the different sizes, shapes and crystallographic orientations. A secondary electron microscope image of the surface of Au polycrystalline substrate was depicted in Fig. 8. Moreover, the diffusion coefficient is a function of concentration, time and position. Nevertheless the derived discrete diffusion profile was the average concentration of Al and Au atoms in a thin slice parallel to the sample surface as a function of depth.

There isn't significant change of the concentration profile after short heating of the sample at − 50 °C for one minute. On the other hand, there is considerable increase of the $Au(4f)_{alloy}/Au(4f)_{metal}$ peak ratio which indicated the gradual growth of the initial AlAu intermetallic phase (see Fig. 2). We tentatively attribute this behaviour to the fast surface reaction of Al and Au atoms which retards the penetration of Al material into Au substrate.

In order to stabilize the in-depth distribution of constituents in the sub-surface region, the sample underwent the prolonged heating at the room temperature promoting the rapid growth of the parent alloy phase. The calculated concentration profiles showed the depletion of Al atoms and enrichment with Au atoms in the sub-surface region of the sample (graph 3 in Fig. 5). This tendency results from

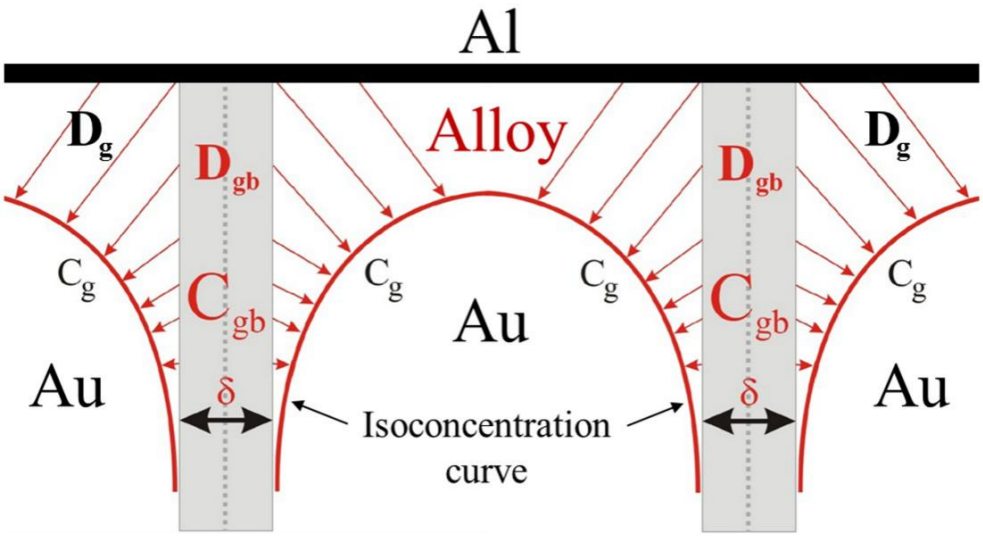

Fig. 7 Schematic representation of the grain boundary model of Al atom diffusion into Au polycrystalline substrate.

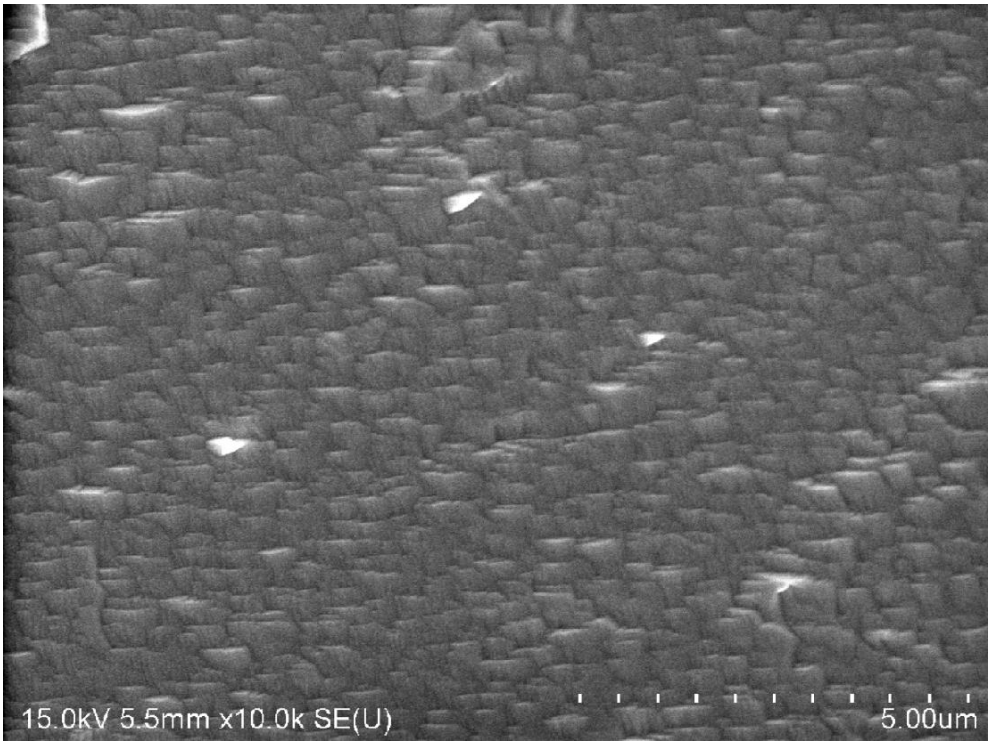

Fig. 8 SEM image of the surface of Au polycrystalline substrate.

the decreasing amount of Al material on Au substrate due to the penetration of Al atoms further into Au bulk. The decreasing tendency of the in-depth profiles can also be associated with the fact that Tikhonov regularization forces down the values of the concentration profile for the depths greater than about 2λ or so, leading to the unreliable data in this region [14].

Hence, all calculated concentration profiles decrease monotonically with depth what is in the reasonable agreement with expected distribution of Al atoms in the sample sub-surface region resulting from the initial localization of Al and Au atoms.

4. Conclusions

ARXPS has proved to be a powerful and reliable

method for the non-destructive probing of the Al/Au interface: extracting chemical state information, in-depth profile estimation, monitoring of interdiffusion, phase growth and phase transformation in real time. ARXPS measurements were performed on the vacuum deposited aluminium of the different amounts on the polycrystalline gold substrate kept at the temperature of liquid nitrogen and during the sample thermal treatments. Our results show that Al atoms interact with Au atoms to form the bimetallic phase even already at the temperature of liquid nitrogen. The Au(4f) line binding energy shift of the initial formed alloy phase has the value of 1.5 eV with respect to the pure gold indicating the formation of AuAl alloy phase. The concentration in-depth profiles of Al constituent into Au substrate were extracted from our ARXPS measurements. The Tikhonov regularization was applied to overcome the ambiguity of solutions that is encountered when the profiles are restored from the real data containing noise. The calculated concentration profiles are in accordance with the expected distribution of Al and Au atoms at the Al/Au interface region resulting from the initial configuration of Al deposit on Au substrate. Prolonged heating of the sample led to the gradual decomposition of the parent AlAu alloy phase and growth of the $AlAu_2$ alloy phase which is richer in Au atoms. Further experimental work on the Al/Au interface formation is necessary to provide a better insight into the solid-state reactions in Al-Au bimetallic couples.

Acknowledgement

The author thanks Dr. Z. Bastl for his comments on the manuscript.

References

[1] Harman, G. G. 1997. "Wire Bonding Microelectronics Materials, Processes, Reliability, Yield." McGraw-Hill.

[2] Piao, H., McIntyre, N. S., Beamson, G., Abel, M.-L. and Watts, J. F. 2002. "Electronic Structures of Au-Al Thin-Film Alloys by High-Energy XPS and XANES." *J. Electron Spectrosc. Relat. Phenom.* 125: 35-45.

[3] Passagrilli, C., Gobbato, L. and Tiziani, R. 2002. "Reliability of Au/Al Bonding in Plastic Packages for High Temperature (200 °C) and High Current Applications." *Microelectron. Reliab.* 42: 1523-8.

[4] Noolu, N. J., Murdeshwar, N. M., Ely, K. J., Lippold, J. C. and Baeslack III, W. A. 2004. "Degradation and Failure Mechanisms in Thermally Exposed Au-Al Ball Bonds." *J. Mat. Res.* 19 (5): 1374-86.

[5] Zhang, X. and Tee, T. Y. 2006. "Numerical and Experimental Correlation of High Temperature Reliability of Gold Wire Bonding to Intermetallics (Au/Al) Uniformity." *Thin Solid Films* 504: 355-61.

[6] Campisano, S. U., Foti, G., Ramini, E., Lau, S. S. and Mayer, J. W. 1975. "Kinetics of Phase Formation in Au-Al Thin Films." *Philos. Mag.* 31: 903-17.

[7] Majni, G., Nobili, C., Ottaviani, G., Costato, M. and Galli, E. 1981. "Gold-Aluminum Thin-Film Interactions and Compound Formation." *J. Appl. Phys.* 52: 4047-54.

[8] Xu, C., Sritharan, T. and Mhaisalkar, S. G. 2007. "Interface Transformations in Thin Film Aluminum – Gold Diffusion Couples." *Thin Solid Films* 515: 5454-61.

[9] Xu, C., Sritharan, T. and Mhaisalkar, S. G. 2007. "Thin Film Aluminum – Gold Interface Interactions." *Scripta Mater.* 56: 549-52.

[10] Pretorius, R., Theron, C. C., Vantomme, A. and Mayer, J. V. 1999. "Compound Phase Formation in Thin Film Structures." *Critical Rev. in Solid State and Mater. Sci.* 24 (1): 1-62.

[11] Fuggle, J. C., Källne, E., Watson, L. M. and Fabian, D. J. 1977. "Electronic Structure of Aluminum and Aluminum-Noble-Metal Alloys Studied by Soft-X-Ray and X-Ray Photoelectron Spectroscopies." *Phys. Rev. B* 16: 750-61.

[12] Piao, H. and McIntyre, N. S. 2001. "High-Resolution Valence Band XPS Studies of Thin Film Au-Al Alloys." *J. Electron Spectrosc. Relat. Phenom.* 119: 29-33.

[13] Sritharan, T., Li, Y. B., Xu, C. and Zhang, S. 2008. "Oxidation of Al-Au Intermetallics and Its Consequences Studied by X-Ray Photoelectron Spectroscopy." *J. Mater. Res.* 23 (5): 1371-82.

[14] Cumpson, P. J. 1995. "Angle-Resolved XPS and AES: Depth-Resolution Limits and a General Comparison of Properties of Depth-Profile Reconstruction Methods." *J. Electron Spectrosc. Relat. Phenom.* 73: 25-52.

[15] Petrov, G. M. 2002. "A Simple Algorithm for Spectral Line Deconvolution." *J. Quant. Spectrosc. Radiat. Transfer.* 72: 281-7.

[16] Hricovini, K. and Dieska, P. 1986. "Subtraction of Satellites in XPS." *Vacuum* 36: 453-4.

[17] Shirley, D. A. 1972. "High-Resolution X-Ray Photoemission Spectrum of the Valence Bands of Gold."*Phys. Rev. B* 5: 4709-14.

[18] Scofield, J. H. 1976. "Hartree-Slater Subshell

Photoionization Cross-Sections at 1254 and 1487 eV." *J. Electron Spectrosc. Relat. Phenom.*8: 129-37.

[19] Tanuma, S., Powell, C. J. and Penn, D. R. 1994. "Calculations of Electron Inelastic Mean Free Paths." *Surf. Interface Anal.* 21: 165-76.

[20] Polyak, Y., Bastl, Z. 2009. "XPS Study of Early Stages of Al/Au Interface Formation." *Surf. Interface Anal.* 41: 830-3.

[21] Clemens, B. M. and Sinclair, R. 1990. "Metastable Phase Formation in Thin Films and Multilayers." *MRS Bulletin* 15 (2): 19-28.

[22] Ulrich, C. M., Hashibon, A., Svoboda, J., Elsässer, C., Helm, D. and Riedel, H. 2011. "Diffusion Kinetics in Aluminium-Gold Bond Contacts from First-Principles Density Functional Calculations." *Acta Mater.* 59: 7634-44.

[23] Ottaviani, G. 1979. "Review of Binary Alloy Formation by Thin Film Interactions." *J. Vac. Sci. Technol.* 16 (5): 1112-9.

[24] Chang, C. C., Callcott, T. A. and Arakawa, E. T. 1985. "Barrier Diffusion and Optical Properties of the Au-Al_2O_3-Al Thin-Film System." *Phys. Rev. B* 32: 6138-44.

[25] Loisel, B. and Arakawa, E. T. 1980. "Diffusion of Al into Au Thin Films Studied by the ATR Method." *Appl. Opt.* 19: 1959-1962.

[26] Smith, G. C. and Livesey, A. K. "Maximum Entropy: A New approach to Non-Destructive Deconvolution of Depth Profiles from Angle-Dependent XPS." *Surf. Interface Anal.* 19: 175-80.

[27] Livesey, A. K. and Smith, G. C. 1994. "The Determination of Depth Profiles from Angle-Dependent XPS Using Maximum Entropy Data Analysis." *J. Electron Spectrosc. Relat. Phenom.* 67: 439-61.

[28] Ebel, H., Ebel, M. F., Wernisch, J. and Jablonski, A. 1984. "The Influence of Elastic Scattering of Electrons on Measured X-Ray Photoelectron Signals." *J. Electron Spectrosc. Relat. Phenom.* 34: 355-62.

[29] Hansen, P. C. 1994. "Regularization Tools: A Matlab Package for Analysis and Solution of Discrete Ill-Posed Problems." *Numerical Algorithms* 6: 1-35.

[30] Peykova, D. and Paynter, R. W. 2012. "Matrix-Based Approach for the Inversion of ARXPS Data." *J. Electron Spectrosc. Relat. Phenom.* 185: 103-11.

[31] Hansen, P. C. 1992. "Analysis of Discrete Ill-Posed Problems by Means of the L-Curve." *SIAM Rev.* 34: 561-80.

[32] Chanbi, Z. and Paynter, R. W. 2008. "On the Choice of the Regularization Parameter for the Interpretation of ARXPS Data Using a Multilayer Model." *J. Electron Spectrosc. Relat. Phenom.* 164: 28-33.

[33] Suzuoka, T. 1961. "Lattice and Grain Boundary Diffusion in Polycrystals." *Trans. Jap. Inst. Met.* 2: 25-32.